

Anisotropic upper critical field and possible Fulde-Ferrel-Larkin-Ovchinnikov state in the stoichiometric pnictide superconductor LiFeAs

K. Cho,¹ H. Kim,^{1,2} M. A. Tanatar,¹ Y. J. Song,³ Y. S. Kwon,³ W. A. Coniglio,⁴ C. C. Agosta,⁴ A. Gurevich,⁵ and R. Prozorov^{1,2,*}

¹Ames Laboratory, Ames, Iowa 50011, USA

²Department of Physics & Astronomy, Iowa State University, Ames, Iowa 50011, USA

³Department of Physics, Sungkyunkwan University, Suwon, Gyeonggi-Do 440-746, Republic of Korea

⁴Department of Physics, Clark University, Worcester, Massachusetts 01610, USA

⁵National High Magnetic Field Laboratory, Florida State University, Tallahassee, Florida 32310, USA

(Received 24 November 2010; revised manuscript received 31 December 2010; published 7 February 2011)

Measurements of the temperature and angular dependencies of the upper critical field H_{c2} of a stoichiometric single crystal LiFeAs in pulsed magnetic fields up to 50 T were performed using a tunnel diode resonator. Complete $H_{c2}^{\parallel c}(T)$ and $H_{c2}^{\perp c}(T)$ functions with $H_{c2}^{\parallel c}(0) = 17 \pm 1$ T, $H_{c2}^{\perp c}(0) = 26 \pm 1$ T, and the anisotropy parameter $\gamma_H(T) \equiv H_{c2}^{\perp c}/H_{c2}^{\parallel c}$ decreasing from 2.5 at T_c to 1.5 at $T \ll T_c$ were obtained. The results for both orientations are in excellent agreement with a theory of H_{c2} for two-band s^{\pm} pairing in the clean limit. We show that $H_{c2}^{\parallel c}(T)$ is mostly limited by the orbital pair breaking, whereas the shape of $H_{c2}^{\perp c}(T)$ indicates strong paramagnetic Pauli limiting and the inhomogeneous Fulde-Ferrel-Larkin-Ovchinnikov state below $T_F \sim 5$ K.

DOI: 10.1103/PhysRevB.83.060502

PACS number(s): 74.70.Xa, 74.25.Ha, 74.25.Op

There are only a few stoichiometric iron-based compounds (Fe-SCs) exhibiting ambient-pressure superconductivity without doping. Among them, LiFeAs is unique because of its relatively high $T_c = 18$ K,¹ as compared to LaFePO ($T_c = 5.6$ K)² and KFe₂As₂ ($T_c = 3$ K).³ The absence of doping-induced disorder leads to weak electron scattering, low resistivity, $\rho(T_c) \approx 10 \mu\Omega$ cm (Ref. 4) and high resistivity ratio, $RRR = \rho(300\text{K})/\rho(T_c) > 30$.^{4,5} These parameters differ significantly from those of most Fe-SCs for which superconductivity is induced by doping, for example, Ba(Fe_{1-x}T_x)₂As₂ (Refs. 6 and 7), (Ba_{1-x}K_x)Fe₂As₂ (Ref. 3), and BaFe₂(As_{1-x}P_x)₂ (Ref. 8). With the highest T_c among stoichiometric Fe-SCs, negative dT_c/dP ,⁹ tetragonal crystal structure,^{1,5} and the absence of antiferromagnetism,¹⁰ LiFeAs serves as a model of clean, nearly optimally doped Fe-SC.⁴ Because of very high H_{c2} of Fe-SCs, they may also exhibit exotic behavior caused by strong magnetic fields, for example, the Fulde-Ferrel-Larkin-Ovchinnikov (FFLO) state in which the Zeeman splitting results in oscillations of the order parameter along the field direction.¹¹ Thus, measurements of $H_{c2}(T)$ in stoichiometric LiFeAs single crystals can reveal manifestations of s^{\pm} pairing in the clean limit¹² for which the FFLO state is least suppressed by doping-induced disorder¹¹ as compared to other optimally doped Fe-SCs.

Measurements of the upper critical fields parallel ($H_{c2}^{\parallel c}$) and perpendicular ($H_{c2}^{\perp c}$) to the crystallographic c axis in many Fe-SCs have shown several common trends.^{6,7,13-27} Close to T_c where H_{c2} is limited by orbital pair breaking, the anisotropy parameter $\gamma_H \equiv H_{c2}^{\perp c}/H_{c2}^{\parallel c}$ ranges between 1.5 and 5,^{13,18,23-26} in agreement with the anisotropy of the normal state resistivity $\gamma_H = (\rho_c/\rho_{ab})^{1/2}$ above T_c .⁷ As T decreases, $H_{c2}(T)$ becomes more isotropic,^{18,20,27} consistent with multiband pairing scenarios and the behavior of H_{c2} in dirty MgB₂,²⁸ yet opposite to clean s^{++} MgB₂ single crystals.²⁹ However, the more isotropic H_{c2} at low T can also result from strong Pauli pair breaking for $\mathbf{H} \parallel ab$, since the observed H_{c2} on many Fe-SCs significantly exceeds the BCS paramagnetic

limit $H_p[T] = 1.84T_c[K]$.^{17,18,25-27,30} Thus, measuring H_{c2} in LiFeAs can probe the interplay of orbital and Pauli pair breaking in the clean s^{\pm} pairing limit at high magnetic fields. These measurements are also interesting because magnetic fluctuations may contain significant ferromagnetic contribution which may lead to triplet pairing.³¹ Experimentally, vortex properties of LiFeAs were found to be very similar to the supposedly triplet Sr₂RuO₄,³² although NMR studies suggest singlet pairing.³³ Triplet superconductors can exhibit unusual responses to a magnetic field,³⁴ and, indeed, candidate materials show pronounced anomalies, as observed in UPt₃ (Refs. 35 and 36) and Sr₂RuO₄ (Ref. 37). Surprisingly, our measurements show that normalized $H_{c2}^{\perp c}$ of LiFeAs matches quite closely that of Sr₂RuO₄.

We present the measurements of a complete H - T phase diagram of LiFeAs in pulsed magnetic fields up to 50 T and down to 0.6 K using a tunnel diode resonator (TDR) technique. We found that $H_{c2}^{\perp c}(T)$ shows rapid saturation at low temperatures, consistent with strong Pauli pair breaking. A similar conclusion was reached from torque measurements.³⁸ Our data can be described well by a theory of H_{c2} for the multiband s^{\pm} pairing in the clean limit,³⁹ which also suggests the FFLO state in LiFeAs for $H \perp c$ below 5 K. Previous measurements of H_{c2} in LiFeAs were performed at relatively low fields,^{5,40} thus not allowing to reveal the spin-limited behavior at low T . The only reported high-field measurements associate H_{c2} with the disappearance of irreversibility in torque measurements.³⁸ The authors supported this association by comparing with the specific heat data. However, in our opinion, the irreversibility field may underestimate the true $H_{c2}(T)$ and have different temperature dependence due to depinning of vortices. It may also have significant (cusplike) angular variation, which would be particularly important for torque measurements that rely on the finite angle between magnetic moment and field. Related complications were discussed in high- T_c cuprates.⁴¹

Single crystals of LiFeAs were grown in a sealed tungsten crucible using the Bridgman method and placed in ampoules.

Immediately after opening, samples were covered with Apiezon N grease, which provides some degree of short-term protection.⁴ The samples were cleaved and cut inside the grease layer to minimize exposure to the air. The two studied samples had dimensions of $0.6 \times 0.5 \times 0.1 \text{ mm}^3$ (sample A) and $0.9 \times 0.8 \times 0.2 \text{ mm}^3$ (sample B). The superconducting transition temperature for both samples was $T_c = 17.6 \pm 0.1 \text{ K}$ (more than 10% higher than $T_c = 15.5 \text{ K}$ of Ref. 38). (Full transition curves of samples from the same batch are presented in Ref. 4.) Dynamic magnetic susceptibility χ was measured with 190-MHz (sample A) and 16-MHz (sample B) TDR.⁴² The magnetic field was generated by a 50-T pulsed magnet with a 11-ms rise time at Clark University. A single-axis rotator with a 0.5° angular resolution was used to accurately align the sample with respect to the magnetic field [see inset in Fig. 2(a)]. The data have been taken for each orientation at temperatures down to 0.66 K. The normal-state data at 25 K have also been taken for both orientations and subtracted. Measured shift of the resonant frequency $\Delta f \propto \chi$ (Ref. 42), thus exhibits a kink at H_{c2} where London penetration depth diverges and is replaced by the normal-state skin depth. Thus, barring uncertainty due to fluctuations, it is probing a “true” upper critical field.

There are only two data points obtained from the second crystal (sample B). Due to lack of high-field magnet time, we could not finish the whole phase diagram for this sample. However, two data points were obtained at the lowest temperature of 0.66 K and are fully consistent with those from sample A. The transition temperature in zero field was nearly identical between the two samples (17.5 and 17.6 K, respectively). These two observations provide a strong confirmation of the reproducibility of the $H_{c2}(T)$ functions.

Drawing two lines to obtain H_{c2} is a common technique in high-field measurement. It has been pointed out that frequency versus field traces are quite rounded leading to some arbitrariness especially at high temperatures. Therefore, we carefully repeated this process many times and consistently from low to high temperatures. In this way the appropriate error bars were obtained for each trace. The data obtained at high temperature, where we had an overlap with conventional magnets, are in a good agreement.

Figure 1 shows the change of the resonant frequency as a function of H for sample A for two field orientations and two temperatures and also shows a graphical definition of H_{c2} . We note that we obtain the same values of H_{c2} from pulse and conventional magnet measurements (up to 9 T) at higher temperatures. From many such traces, both $H_{c2}^{\perp c}$ and $H_{c2}^{\parallel c}$ were determined as shown in Fig. 1 and are plotted in Fig. 2. Only lowest temperature pulse field sweeps as well as an $H = 0$ temperature sweep were measured for sample B. The results practically coincide with the data for sample A.

Figure 2(a) compares our H_{c2} data on samples A and B with the previous transport^{5,40,43} and torque measurements.³⁸ Figure 2(a) also shows the behavior expected from the orbital Werthamer-Helfand-Hohenberg (WHH) theory⁴⁴ with $H_{\text{orb}}(0) = 0.69T_c[dH_{c2}/dT]|_{T_c}$, the single-gap BCS paramagnetic limit, $H_p^{\text{BCS}} = 1.84T_c = 32.2 \text{ T}$, as well as $H_p^{\Delta_1} = 34.7 \text{ T}$ and $H_p^{\Delta_2} = 20.4 \text{ T}$ calculated with $\Delta_1(0)/T_c \approx 1.885$ and $\Delta_1(0)/T_c \approx 1.111$ reported for the same samples in Ref. 4. Clearly, the observed $H_{c2}(T)$ exhibits much stronger

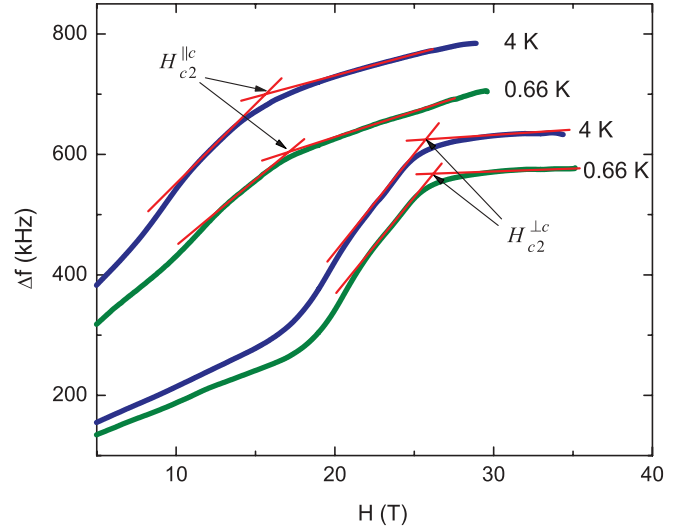


FIG. 1. (Color online) TDR frequency change for increasing pulsed magnetic field, applied in two orientations, $H \parallel c$ and $H \perp c$, shown for two temperatures for sample A. The definition of H_{c2} is shown as the intersection of two straight lines below and above the transition.

flattening at low temperature compared to the orbital WHH theory. The inset in Fig. 2(a) shows the dependence of H_{c2} on the angle φ between \mathbf{H} and the ab plane at 0.66 K where $H_{c2}^{\perp c}$ is defined at a maximum of $H_{c2}(\varphi) = H_{c2}^{\parallel c} + (H_{c2}^{\perp c} - H_{c2}^{\parallel c}) \cos \varphi$ depicted by the solid line.

We analyze our $H_{c2}(T)$ data using a two-band theory, which takes into account both orbital and paramagnetic pair breaking in the clean limit, and the possibility of the FFLO with the wave vector $\mathbf{Q}(T, H)$. In this case the equation for H_{c2} is given by³⁹

$$a_1 G_1 + a_2 G_2 + G_1 G_2 = 0, \quad (1)$$

$$G_1 = \ln t + 2e^{q^2} \text{Re} \sum_{n=0}^{\infty} \int_q^{\infty} du e^{-u^2} \times \left[\frac{u}{n+1/2} - \frac{t}{\sqrt{b}} \tan^{-1} \left(\frac{u\sqrt{b}}{t(n+1/2) + i\alpha b} \right) \right]. \quad (2)$$

Here $Q(T, H)$ is determined by the condition that $H_{c2}(T, Q)$ is maximum, $a_1 = (\lambda_0 + \lambda_-)/2w$, $a_2 = (\lambda_0 - \lambda_-)/2w$, $\lambda_- = \lambda_{11} - \lambda_{22}$, $\lambda_0 = (\lambda_-^2 + 4\lambda_{12}\lambda_{21})^{1/2}$, $w = \lambda_{11}\lambda_{22} - \lambda_{12}\lambda_{21}$, $t = T/T_c$, and G_2 is obtained by replacing $\sqrt{b} \rightarrow \sqrt{\eta b}$ and $q \rightarrow q\sqrt{s}$ in G_1 , where

$$b = \frac{\hbar^2 v_1^2 H}{8\pi \phi_0 k_B^2 T_c^2 g_1^2}, \quad \alpha = \frac{4\mu \phi_0 g_1 k_B T_c}{\hbar^2 v_1^2}, \quad (3)$$

$$q^2 = Q_z^2 \phi_0 \epsilon_1 / 2\pi H, \quad \eta = v_2^2 / v_1^2, \quad s = \epsilon_2 / \epsilon_1. \quad (4)$$

Here, v_l is the in-plane Fermi velocity in band $l = 1, 2$, $\epsilon_l = m_l^{ab}/m_l^c$ is the mass anisotropy ratio, ϕ_0 is the flux quantum, μ is the magnetic moment of a quasiparticle, λ_{11} and λ_{22} are the intraband pairing constants, λ_{12} and λ_{21} are the interband pairing constants, and $\alpha \approx 0.56\alpha_M$ where the Maki parameter $\alpha_M = \sqrt{2}H_{c2}^{\text{orb}}/H_p$ quantifies the strength of the Zeeman pair breaking. The factors $g_1 = 1 + \lambda_{11} + |\lambda_{12}|$ and $g_2 = 1 + \lambda_{22} + |\lambda_{21}|$ describe the strong coupling Eliashberg corrections. For

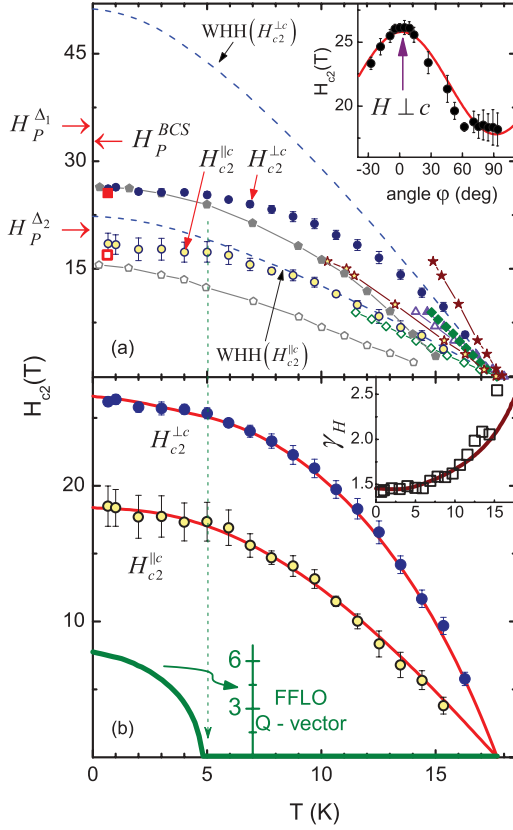


FIG. 2. (Color online) (a) $H_{c2}(T)$ for $H \perp c$ (solid symbols) and $H \parallel c$ (open symbols). Blue circles and red squares correspond to samples A and B, respectively. For comparison we show the literature data determined from the resistivity measurements with midpoint criterion: (magenta) triangles,⁵ (green) rhombi,⁴⁰ (brown) stars.⁴³ Torque data are shown by (grey) pentagons.³⁸ Dashed lines are the WHH $H_{c2}(T)$. Inset in (a) shows $H_{c2}(\varphi)$ at 0.66 K where the solid line is $H_{c2}(\varphi) = H_{c2}^{\parallel c} + (H_{c2}^{\perp c} - H_{c2}^{\parallel c}) \cos \varphi$. (b) Fit of the experimental data to $H_{c2}(T)$, $Q(T)$, and $\gamma_H(T)$ (solid lines) calculated from Eq. (1) for the parameters given in the text. The FFLO wave vector $Q(T)$ is plotted in the units of $40\pi k_B T_c g_1 / \hbar v_1$, and the inset shows $\gamma_H(T)$.

the sake of simplicity, we consider here the case of $\epsilon_1 = \epsilon_2 = \epsilon$ for which $H_{c2}^{\perp c}$ is defined by Eqs. (1) and (2) with $g_1 = g_2$ and rescaled $q \rightarrow q\epsilon^{-3/4}$, $\alpha \rightarrow \alpha\epsilon^{-1/2}$, and $\sqrt{b} \rightarrow \epsilon^{1/4}\sqrt{b}$ in G_1 and $\sqrt{\eta b} \rightarrow \epsilon^{1/4}\sqrt{\eta b}$ in G_2 .³⁹

Figure 2(b) shows the fit of the measured $H_{c2}(T)$ to Eq. (1) for s^{\pm} pairing with $\lambda_{11} = \lambda_{22} = 0$, $\lambda_{12}\lambda_{21} = 0.25$, $\eta = 0.3$, $\alpha = 0.35$, and $\epsilon = 0.128$. Equation (1) describes $H_{c2}^{\parallel c}(T)$, $H_{c2}^{\perp c}(T)$ and $\gamma_H(T) = b_{\parallel}(T)/\sqrt{\epsilon}b_{\perp}(T)$ where $b_{\parallel}(T)$ and $b_{\perp}(T)$ are the solutions of Eq. (1) for $H \parallel c$ and $H \perp c$, very well. The fit parameters are also in good quantitative agreement with experiment. For instance, the Fermi velocity $v_1 = (g_1 k_B T_c / \hbar)[8\pi\phi_0 b_{\perp}(0)/H_{c2}^{\parallel c}(0)]^{1/2}$ can be expressed from Eq. (4) in terms of material parameters and $b_{\perp}(0) = 0.314$ calculated from Eq. (1). For $T_c = 17.8$ K, $H_{c2}^{\parallel c}(0) = 18.4$ T, and $g = 1.5$ for $\lambda_{12} = 0.5$, we obtain $v_1 = 1.12 \times 10^7$ cm/s, consistent with the ARPES results.¹⁰

Several important conclusions follow from the results shown in Fig. 2(b). First, contrary to the single-band Ginzburg-Landau scaling, $\gamma_H^{\text{GL}} = \epsilon^{-1/2}$, the anisotropy parameter $\gamma_H(T)$

decreases as T decreases. Not only is this behavior indicative of multiband pairing,²⁸ but it also reflects the significant role of the Zeeman pair breaking in LiFeAs given that $\alpha_{\parallel} = \alpha/\sqrt{\epsilon} = 0.98$ for $H \perp c$ is close to the single-band FFLO instability threshold, $\alpha \approx 1$.³⁹ In this case, $\gamma_H(T)$ near T_c is determined by the orbital pair breaking and the mass anisotropy ϵ , but as T decreases, the contribution of the isotropic Zeeman pair breaking increases, resulting in the decrease of $\gamma_H(T)$. Another intriguing result is that the solution of Eq. (1) shows no FFLO instability for $H \parallel c$, but predicts the FFLO transition at $T < T_F \approx 5$ K for $H \parallel ab$. Similar to organic superconductors,⁴⁵ this temperature is notably lower than $T_F = 0.56T_c$ ⁴⁶ expected for a single band in the limit of no orbital pairbreaking ($\alpha \rightarrow \infty$). The FFLO wave vector $Q(T) = 4\pi k_B T_c q(T)b^{1/2}(T)g_1/\hbar v_1$ appears spontaneously at $T = T_F \approx 5$ K where the FFLO period $\ell = 2\pi/Q = \hbar v_1/2k_B T_c g_1 q(T)b^{1/2}(T)$ diverges and then decreases as T decreases, reaching $\ell(0) = \pi\xi_0/g_1 q(0)b^{1/2}(0) \approx 9\xi_0$ at $T = 0$. Here $q(0) = 0.656$, $b(0) = 0.126$, and $\xi_0 = \hbar v_1/2\pi k_B T_c \simeq 7.3$ nm, giving $\ell(0) \simeq 65.6$ nm for the parameters used above. The period $\ell(0)$ is much smaller than the mean free path, $\ell_{\text{mfp}} \sim 550$ nm, estimated from the Drude formula for an ellipsoidal Fermi surface with $\epsilon = 0.128$, $v_F = 112$ km/s, m_{ab} equal to the free electron mass, and $\rho(T_c) = 10\mu\Omega$ cm. Notice that $\rho(T_c)$ may contain a significant contribution from inelastic scattering, so the mean free path for elastic impurity scattering which destroys the FFLO state¹¹ is even larger than ℓ_{mfp} . Therefore, the FFLO state predicted by our calculations may be a realistic possibility verifiable by specific heat, magnetic torque, and thermal conductivity measurements. Magnetic measurements³⁸ have revealed a jump in the torque developing below ~ 8 K, consistent with the first order FFLO transition.

Finally, we compare LiFeAs with other superconductors, especially those for which H_{c2} is clearly limited

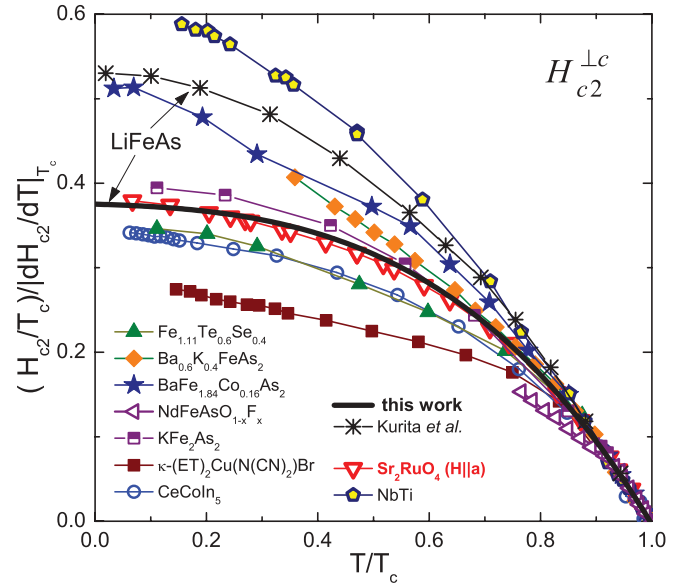


FIG. 3. (Color online) $(H_{c2}(T)/T_c)/|dH_{c2}/dT|_{T_c}$ vs T/T_c in the $H \perp c$ orientation. Black solid line is our data in comparison with several Fe-SCs as well as other exotic superconductors and conventional NbTi, all shown in the legend.

by either orbital or Zeeman pair breaking. Shown in Fig. 3 are the normalized $H_{c2}(T)/T_c H'_{c2}$ as functions of T/T_c for $\mathbf{H} \parallel ab$ where the Zeeman pair breaking is most pronounced. Here $H'_{c2} = |dH_{c2}/dT|_{T \rightarrow T_c}$, and our data are shown by the thick solid black line, whereas the literature data are shown by symbols. The reference materials include LiFeAs;³⁸ Pauli-limited⁴⁷ organic superconductor κ -(BEDT-TTF)₂Cu[N(CN)₂]Br;⁴⁸ heavy fermion CeCoIn₅;⁴⁹ optimally doped iron pnictides, Ba(Fe_{1-x}Co_x)₂As₂ (Ref. 18) and Ba_xK_{1-x}FeAs₂;²⁰ iron chalcogenide Fe(Se,Te);²⁷ and conventional NbTi.⁵⁰ Remarkably, scaled data obtained on crystals with different T_c and by different measurements (this work and Ref. 38) are very similar, indicating an intrinsic behavior of LiFeAs, namely, that it is indeed closer to the paramagnetic limit. Notably, the data for LiFeAs lay below other Fe-SCs, except for the highest purity ($RRR \approx 87$) KFe₂As₂.⁵¹ On the other hand, our data appear above CeCoIn₅, believed to be mostly Pauli limited.⁴⁹ Interestingly, the data for LiFeAs stay almost on top of the $H_{c2}(T)$ for Sr₂RuO₄, in which limiting of H_{c2} proceeds in a very unusual manner, leading to the formation of the second superconducting phase.³⁷ Given that vortex dynamics in these two materials is also similar,³²

the coincidence of the $H_{c2}(T)/T_c H'_{c2}$ curves is worth further exploration.

Summarizing. Full-temperature-range experimental $H_{c2}^{\parallel c}(T)$ and $H_{c2}^{\perp c}(T)$ deviate significantly from the single-band WHH behavior but are in excellent agreement with the theory of H_{c2} for the s^{\pm} pairing in the clean limit. Our results indicate Pauli-limited behavior and the FFLO state below 5 K for $H \perp c$.

We thank A. Carrington, V. G. Kogan, L. Taillefer and T. Terashima for discussions. The work at Ames Laboratory was supported by the US Department of Energy, Office of Basic Energy Sciences, Division of Materials Sciences and Engineering under Contract No. DE-AC02-07CH11358. The work at Clark was supported by the US Department of Energy under Contract No. ER46214. The work at Sungkyunkwan University was supported by the Basic Science Research Program (2010-0007487), the Mid-career Researcher Program (No. R01-2008-000-20586-0). R.P. acknowledges support from the Alfred P. Sloan Foundation. A.G. was supported by NSF through NSF-DMR-0084173 and by the State of Florida.

*Corresponding author: prozorov@ameslab.gov

¹X. C. Wang *et al.*, *Solid State Comm.* **148**, 538 (2008).

²Y. Kamihara *et al.*, *J. Am. Chem. Soc.* **128**, 10012 (2006).

³M. Rotter *et al.*, *Phys. Rev. Lett.* **101**, 107006 (2008).

⁴H. Kim *et al.*, e-print arXiv:1008.3251.

⁵Y. J. Song *et al.*, *Appl. Phys. Lett.* **96**, 212508 (2010).

⁶N. Ni *et al.*, *Phys. Rev. B* **82**, 024519 (2010).

⁷M. A. Tanatar *et al.*, *Phys. Rev. B* **79**, 094507 (2009).

⁸S. Kasahara *et al.*, *Phys. Rev. B* **81**, 184519 (2010).

⁹C. W. Chu *et al.*, *Physica C* **469**, 326 (2009).

¹⁰S. V. Borisenko *et al.*, *Phys. Rev. Lett.* **105**, 067002 (2010).

¹¹Y. Matsuda and H. Shimahara, *J. Phys. Soc. Jpn.* **76**, 051005 (2007).

¹²I. Mazin *et al.*, *Phys. Rev. Lett.* **101**, 057003 (2008); K. Kuroki *et al.*, *ibid.* **101**, 087004 (2008); V. Mishra *et al.*, *Phys. Rev. B* **79**, 094512 (2009).

¹³F. Hunte *et al.*, *Nature (London)* **453**, 903 (2008).

¹⁴Y. Jia *et al.*, *Appl. Phys. Lett.* **93**, 032503 (2008).

¹⁵J. Kacmarcik *et al.*, *Phys. Rev. B* **80**, 014515 (2009).

¹⁶H. Lee *et al.*, *Phys. Rev. B* **80**, 144512 (2009).

¹⁷J. Jaroszynski *et al.*, *Phys. Rev. B* **78**, 174523 (2008).

¹⁸M. Kano *et al.*, *J. Phys. Soc. Jpn* **78**, 084719 (2009).

¹⁹Z. Bukowski *et al.*, *Phys. Rev. B* **79**, 104521 (2009).

²⁰H. Q. Yuan *et al.*, *Nature (London)* **457**, 565 (2009).

²¹S. Jiang *et al.*, *Phys. Rev. B* **80**, 184514 (2009).

²²N. P. Butch *et al.*, *Phys. Rev. B* **81**, 024518 (2010).

²³D. Braithwaite *et al.*, *J. Phys. Soc. Jpn.* **79**, 053703 (2010).

²⁴H. Lei *et al.*, *Phys. Rev. B* **81**, 184522 (2010).

²⁵T. Kida *et al.*, *J. Phys. Soc. Jpn.* **79**, 074706 (2010).

²⁶S. Khim *et al.*, *Phys. Rev. B* **81**, 184511 (2010).

²⁷M. Fang *et al.*, *Phys. Rev. B* **81**, 020509(R) (2010).

²⁸A. Gurevich, *Phys. Rev. B* **67**, 184515 (2003).

²⁹V. G. Kogan and S. L. Bud'ko, *Physica C* **385**, 131 (2003).

³⁰G. Fuchs *et al.*, *Phys. Rev. Lett.* **101**, 237003 (2008); *New J. Phys.* **11**, 075007 (2009); A. Yamamoto *et al.*, *Appl. Phys. Lett.* **94**, 062511 (2009); M. Altarawneh *et al.*, *Phys. Rev. B* **78**, 220505(R) (2008).

³¹T. M. Rice and M. Sigrist, *J. Phys. Condens. Matter* **7**, L643 (1995).

³²A. K. Pramanik *et al.*, e-print arXiv:1009.4896.

³³Z. Li *et al.*, *J. Phys. Soc. Jpn.* **79**, 083702 (2010).

³⁴A. G. Lebed and N. Hayashi, *Physica C* **341**, 1677 (2000).

³⁵H. Suderow *et al.*, *Phys. Rev. Lett.* **80**, 165 (1998).

³⁶K. Hasselbach *et al.*, *Phys. Rev. Lett.* **63**, 93 (1989).

³⁷K. Deguchi *et al.*, *J. Phys. Soc. Jpn.* **71**, 2839 (2002).

³⁸N. Kurita *et al.*, *J. Phys. Soc. Jpn.* **80**, 013706 (2011).

³⁹A. Gurevich, *Phys. Rev. B* **82**, 184504 (2010).

⁴⁰B. Lee *et al.*, *Europhys. Lett.* **91**, 67002 (2010).

⁴¹A. Carrington *et al.*, *Phys. Rev. B* **54**, 3788 (1996).

⁴²R. Prozorov and R. W. Giannetta, *Supercond. Sci. Technol.* **19**, R41 (2006).

⁴³O. Heyer *et al.*, e-print arXiv:1010.2876.

⁴⁴N. R. Werthamer *et al.*, *Phys. Rev.* **147**, 295 (1966).

⁴⁵M. A. Tanatar *et al.*, *Phys. Rev. B* **66**, 134503 (2002).

⁴⁶L. W. Gruenberg and L. Gunther, *Phys. Rev. Lett.* **16**, 996 (1966).

⁴⁷A. E. Kovalev *et al.*, *Phys. Rev. B* **62**, 103 (2000).

⁴⁸E. Ohmichi *et al.*, *Syn. Metals* **133**, 245 (2003).

⁴⁹A. Bianchi *et al.*, *Phys. Rev. Lett.* **91**, 187004 (2003).

⁵⁰Y. Shapira and L. J. Neuringer, *Phys. Rev.* **140**, A1638 (1965).

⁵¹T. Terashima *et al.*, *J. Phys. Soc. Jpn.* **78**, 063702 (2009).